SvedbergOpen
DISSEMINATION OF KNOWLEDGE

International Journal of Artificial Intelligence and Machine Learning

Publisher's Home Page: https://www.svedbergopen.com/

Research Paper Open Access

Experimental Investigation and Finite Element Validation of Load–Settlement Response of Square Footings on Geogrid-Reinforced Manufactured Sand Beds

Srinivasa RH [1] Dr. S. Gangadhara [2]

[1] Research Scholar, Department of Civil Engineering, University Visvesvaraya College of Engineering (UVCE), Bangalore University, Bengaluru, Karnataka, India – 560056.
[2] Professor, Department of Civil Engineering, University Visvesvaraya College of Engineering (UVCE), Bangalore University, Bengaluru, Karnataka, India - 560056 .

Abstract
Ground improvement techniques are methods used in geotechnical engineering to make weak soil stronger and less compressible so that it can safely support structures. These methods help to increase the bearing capacity of soil and reduce both total and differential settlement. Geogrids form a very effective reinforcement system for weak soils as they add tensile strength and confinement effect. Geogrids are polymer grid elements (uniaxial, biaxial or triaxial) placed in soil so that particles interlock within their apertures, creating a composite soil–geogrid mass with higher stiffness and strength. Manufactured sand (M-sand) plays a significant role as a sustainable alternative to river sand in reinforced foundation systems. Its angularity and rough surface texture promote better mechanical interlocking with geogrid reinforcement, thereby enhancing confinement, increasing bearing capacity, and reducing settlement under static loading conditions. The present study focuses on evaluating the load–settlement response of square footings resting on geogrid-reinforced M-sand beds under static loading conditions through experimental and numerical investigation. The study aims to determine the optimum reinforcement configuration in terms of number of layers and spacing. The results are compared with Bearing capacity ratio and settlement ratio thereby establishing M-sand as a sustainable and high-performance foundation material for infrastructure applications.

1. Introduction

The rapid expansion of infrastructure projects has led to an increasing demand for reliable foundation systems capable of performing satisfactorily even on weak or compressible soils. In many cases, natural soils do not possess adequate strength or stiffness to safely support structural loads, resulting in excessive settlement and potential instability. To address these challenges, ground improvement techniques are widely adopted in geotechnical engineering to modify soil properties and enhance overall foundation performance. Ground improvement methods are primarily aimed at increasing the load-bearing capacity of soil while minimizing both total and differential settlements. Among the various techniques available, the use of geosynthetic reinforcements has gained prominence due to their efficiency, adaptability, and economic advantages. Geogrids, in particular, are extensively used as reinforcement elements because of their ability to provide tensile resistance and improve stress distribution within soil masses. Geogrids are polymeric grid structures available in different configurations such as uniaxial, biaxial, and triaxial forms. When embedded within soil, they interact with surrounding particles through interlocking mechanisms, which enhance confinement and restrict lateral movement. This interaction results in the formation of a composite system with improved stiffness and shear strength. Consequently, geogrid-reinforced soils exhibit higher bearing capacity and reduced deformation compared to unreinforced conditions. In parallel with reinforcement techniques, the search for sustainable construction materials has led to the increased use of manufactured sand (M-sand) as an alternative to natural river sand. The depletion of river sand resources, coupled with environmental regulations, has accelerated the adoption of M-sand in geotechnical and construction applications. Due to its angular shape and rough surface texture, M-sand provides superior interparticle friction and improved bonding characteristics, which are particularly beneficial when used in conjunction with geogrid reinforcement. This combination enhances the confinement effect and promotes efficient load transfer within the reinforced soil system.

Numerous researchers [5,6,12] have performed experimental investigations to evaluate the role of geogrid reinforcement in improving the bearing capacity of weak soil foundations. In addition, several studies [1–2,15] have adopted numerical approaches to analyze the behaviour of both single-layered and layered soil systems, particularly examining the influence of unstabilized and stabilized clayey layers over medium-dense sand on bearing capacity and failure mechanisms. The findings consistently indicate that the inclusion of geosynthetic reinforcement enhances soil shear strength and effectively reduces settlement. In most numerical simulations, soil behaviour is commonly represented using nonlinear constitutive models such as the Drucker–Prager and Mohr–Coulomb models, while the reinforcement and footing are generally idealized as linear isotropic materials. Parametric investigations [4,13,14] emphasize that the performance of reinforced systems is primarily governed by factors such as the number of reinforcement layers, depth of reinforcement, and spacing between successive layers.Comparative studies involving laboratory model tests on circular footings under static loading conditions demonstrate that numerical predictions obtained using ABAQUS closely match experimental results, considering variations in relative density (30%, 50%, and 70%) and footing diameter (75 mm and 100 mm) [9]. Further numerical analyses reveal that geogrid reinforcement becomes more effective at higher settlement levels (greater than 2%), with optimum placement typically located at approximately one-third of the base thickness from the surface, making it particularly suitable for weak subgrades with low CBR values (<5%) [11,14].Advanced numerical studies on square footings reinforced with three-dimensional geogrids indicate superior performance compared to planar reinforcement and unreinforced cases, with bearing capacity ratios reaching approximately 6.3 for 3D geogrids compared to about 3.7 for planar systems [8]. Moreover, finite element simulations validated through experimental pullout tests confirm that three-dimensional modelling approaches can reliably capture geogrid–soil interaction behaviour [10]. Similarly, numerical modelling using PLAXIS demonstrates that appropriate reinforcement configuration significantly enhances bearing capacity, with optimal parameters reported as u/B = 0.25, h/B = 0.75, L/B = 7.5, and four reinforcement layers, while the bearing capacity ratio increases with the number of layers and decreases with increasing footing width [3]. Previous studies have indicated that the performance of reinforced soil systems is significantly influenced by factors such as the number of reinforcement layers, spacing between layers, and placement depth. However, the optimization of these parameters for M-sand-based reinforced foundations requires further investigation to establish reliable design guidelines. The present study aims to evaluate the load–settlement behaviour of square footings resting on geogrid-reinforced M-sand beds under static loading conditions. Both experimental and numerical approaches are employed to analyse the response of the system and to validate the observed behaviour. The numerical modelling is carried out using finite element analysis to simulate the interaction between soil and reinforcement and to understand the underlying mechanisms governing the system response. In addition, the study focuses on identifying the optimum reinforcement configuration in terms of the number of geogrid layers and their vertical spacing. The performance of the reinforced system is assessed using non-dimensional parameters such as the Bearing Capacity Ratio (BCR) and Settlement Ratio (SR). The findings of this study are expected to demonstrate the effectiveness of geogrid-reinforced M-sand as a sustainable and high-performance solution for foundation systems in modern infrastructure development.

2. Materials and Methodology

2.1 Materials

Back fill material: In the present experimental study, M-Sand (Manufactured sand) is used as back filling material for the reinforced earth. M-Sand Properties are presented in Table 1. According to Indian Standard Soil Classification System (ISSCS) the M-sand used in the present study is classified as poorly graded sand (SP).

Table 1: Physical properties of M-Sand

SL No.	Properties	Test Results
1.	Specific Gravity	2.65
2.	Grain Size Distribution:	
	Sand Size (%)	100
3.	Coefficient of Uniformity, Cu	3.55
4.	Coefficient of Curvature, Cc	0.88
5.	Max. Dry Density, γ_{dmax} (kN/m^3)	19.65
6.	Min. Dry Density, γ_{dmin} (kN/m^3))	15.96
7.	Max. Voids Ratio, e_{max}	0.63
8.	Min. Voids Ratio, e_{min}	0.32

Geogrid: In the present experimental study, a hexagonal geogrid is used as reinforcement material. Table 2 presents the properties of the hexagonal geogrid.

Table 2. Physical properties of geogrid

SL No.	Properties	Test Results

1.	Peak Tensile Strength (kN/m)	7.74
2.	Structure	Biaxial Hexagonal
3.	Aperture size in Horizontal (mm)	25.40
4.	Aperture Size in Vertical (mm)	31.80
5.	Rib thickness (mm)	3.00
6.	Joint thickness (mm)	5.00

2.2 Methodology

Testing Procedure

(a) Static load tests:

Static load experimental set-up consists of a loading frame of capacity 50 kN. A 250 mm diameter plate that moves vertically at a rate of 1.06mm/min is placed as a support to the test tank. A cross-beam is provided above the supporting plate for fixing the proving ring. Loads were applied using a mechanical screw jack through a calibrated proving ring of 50 kN capacity with a least count of 0.0602 kN/div. Three dial guages with sensitivity of 0.01 mm, are used.

(b) Experimental Setup for Static Test

The experimental setup consists of,

1. Mild steel footing of size 100mm × 100mm and thickness of 10 mm
2. Mild steel test tank of 500mm diameter and 390mm height.

Test tank diameter to model footing size ratio of 5 is maintained.

Fig.1 Static Test loading frame

Fig.2.Laboratory test tank

(c) Preparation of Test Sample

For unreinforced condition three equal layer of 120mm thickness bed is compacted at required relative density in test tank upto a height of 360mm. And for the reinforced condition, the geogrids are placed at the predetermined depth in the M-sand bed. Circular shaped geogrids are placed with clearance of 5mm between the geogrid and tank surface in order to ensure there is no friction between the geogrid and steel tank. Footing is placed on the levelled surface of the M-sand bed at the canter of tank (Fig 3). Load tests are conducted on M-sand bed compacted at a relative density of 35%, for the both reinforced and unreinforced conditions.

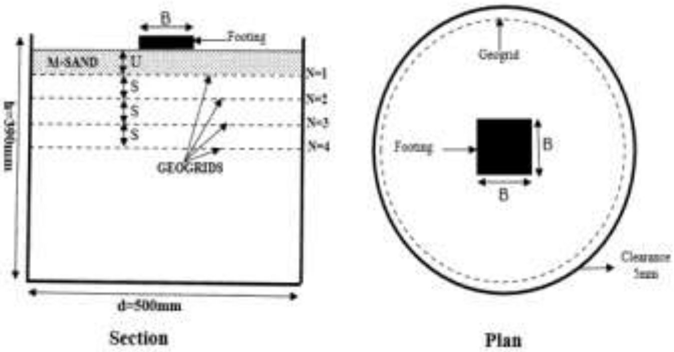

Fig 3. Experimental model footing cross-section and plan

3. Parametric Study

A comprehensive parametric study was carried out using the validated numerical model to investigate the influence of key reinforcement parameters on the performance of square footings resting on geogrid-reinforced M-sand beds. The primary parameters considered include the number of geogrid layers (N=1 to 4), spacing between reinforcement layers (S/B=0.3 to 0.5), and depth of the first reinforcement layer (U/B=0.3 to 0.5). The performance was evaluated in terms of load–settlement response, Bearing Capacity Ratio (BCR), and Settlement Ratio (SR).

4. Results and Discussion

4.1 Effect of depth of first layer of reinforcement.

Laboratory experiments were carried out to identify the optimum depth of the first layer of reinforcement from the bottom of the footing (U) in a reinforced M-sand bed. In the study, tests are conducted for U/B equal to 0.3, 0.4 and 0.5B where B is the size of the footing. Fig.4 presents the pressure-settlement curves for unreinforced and geogrid-reinforced M-sand beds with various U/B ratios (N=1). From the figure, it is observed that the footing resting on an unreinforced M-sand bed shows the bearing pressure of 238kPa at 40mm settlement whereas the footing resting on a reinforced M-sand bed with a single layer of reinforcement (N=1) with U/B=0.3B, 0.4B and 0.5B shows the bearing pressure of 672kPa, 615kPa and 561kPa at 40mm settlement. Thus an improvement of 2.82, 2.58 and 2.35 times improvement is observed in the reinforced M-sand bed with U/B equal to 0.3B, 0.4B and 0.5B, respectively, The maximum improvement in the bearing pressure is observed where the first layer of reinforcement is placed at a depth of 0.3 times the width of footing.

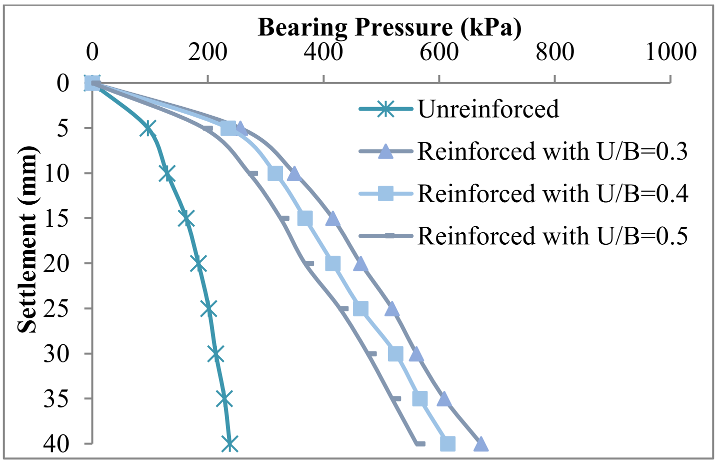

Fig.4 Bearing Pressure-settlement curve for various U/B ratios (N=1)

4.2 Effect of vertical spacing of reinforcement layer (S).

A systematic experimental study was conducted to examine the influence of vertical spacing of geogrid reinforcement (S) on the performance of square footings resting on reinforced M-sand beds. The reinforcement spacing considered were S/B = 0.3, 0.4, and 0.5, where "B" is the size of footing while the depth of the first reinforcement layer was kept constant at U/B = 0.3 for all test cases.Fig.5 presents the pressure–settlement response for unreinforced and two-layer geogrid-reinforced M-sand beds. At a settlement of 40 mm, the unreinforced condition exhibits a bearing pressure of 238 kPa. Upon introducing two layers of geogrid reinforcement, the bearing pressure increases significantly to 1391 kPa, 1108 kPa, and 1026 kPa for reinforcement spacing ratios of 0.3B, 0.4B, and 0.5B, respectively. This clearly demonstrates the beneficial effect of reinforcement, with closer spacing providing greater improvement.

Similar trend of results are observed in Fig 6 and Fig 7. These results shows that the reinforcement spacing ratio of S/B = 0.3 yields the maximum improvement in bearing capacity compared to wider spacings (S=0.4B & 0.5B). This enhancement can be attributed to the increased confinement effect provided by closely spaced geogrid layers, which effectively restrict lateral deformation of the M-sand. In addition, the angular nature of M-sand particles promotes strong mechanical interlocking with the geogrid apertures, resulting in improved shear resistance, more uniform stress distribution, and reduced settlement.

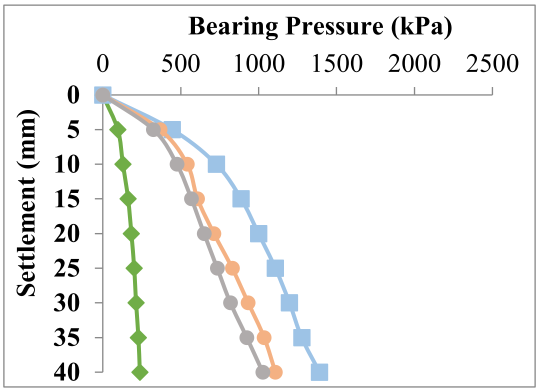

Fig.5 Pressure-settlement curves for square footing resting on 2 layer geogrid reinforced M-Sand Bed

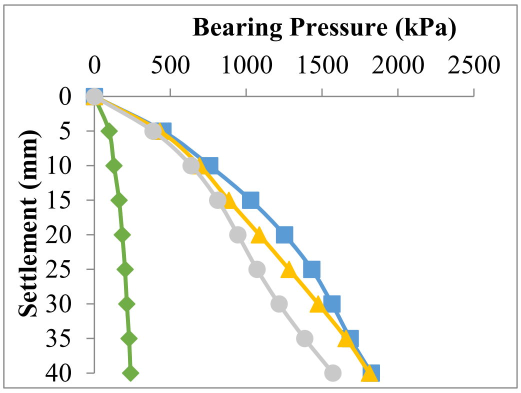

Fig.6 Pressure-settlement curves for square footing resting on 3 layer geogrid reinforced M-Sand Bed

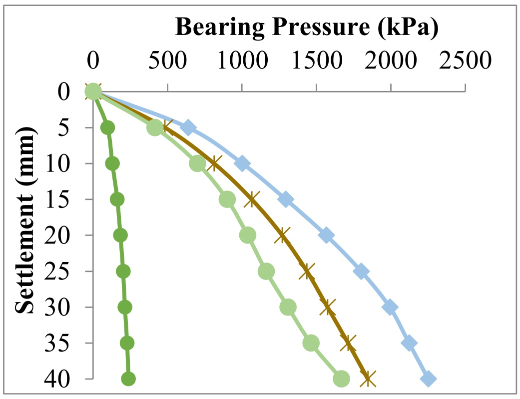

Fig.7 Pressure-settlement curves for square footing resting on 4 layer geogrid reinforced M-Sand Bed

4.3 Effect of number of reinforcement layer (N)

To investigate the influence of the number of geogrid reinforcement layers on the bearing pressure and settlement characteristics, a comprehensive set of experimental analyses was performed on reinforced M-sand beds. In all cases, the depth of the first reinforcement layer was maintained constant at U = 0.3B. Fig.8, Fig. 9, and Fig.10 presents the effect of varying the number of reinforcement layers (N = 0, 2, 3, and 4) on the performance of square footings resting on unreinforced and geogrid-reinforced M-sand beds for spacing ratios of S = 0.3B, 0.4B, and 0.5B, respectively. The results consistently demonstrate that the inclusion of geogrid layers significantly enhances the load-bearing pressure of the footing while reducing settlement. Among all configurations, the case with four layers of reinforcement (N = 4) exhibits the highest bearing pressure and the least settlement. The unreinforced M-sand bed resist a bearing pressure of 238 kPa at a settlement of 40 mm. With the inclusion of geogrid reinforcement at a spacing of S/B = 0.3, the bearing pressure increases significantly to 1391 kPa, 1824 kPa, and 2251 kPa for N = 2, 3, and 4, respectively. Reinforced M-sand with 4 number of reinforcement shows the higher bearing pressure at 40mm settlement compared to all other testing conditions. Similar trend of results is observed in Fig. 8 and Fig 9 for S/B=0.4 and S/B=0.5 respectively. The results indicate a clear trend of increasing bearing presssure with an increase in the number of reinforcement layers, irrespective of the reinforcement spacing. This improvement can be attributed to the enhanced confinement effect provided by multiple geogrid layers, which effectively restricts lateral deformation of the M-sand. The interaction between the geogrid and the angular particles of M-sand promotes efficient load transfer and stress redistribution, leading to improved shear strength and reduced settlement. Overall, the inclusion of multiple geogrid layers significantly improves the performance of M-sand beds, with four layers of reinforcement providing the optimum response under the given conditions.

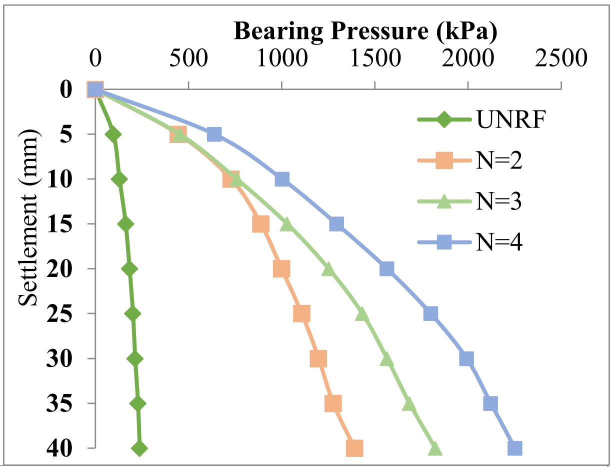

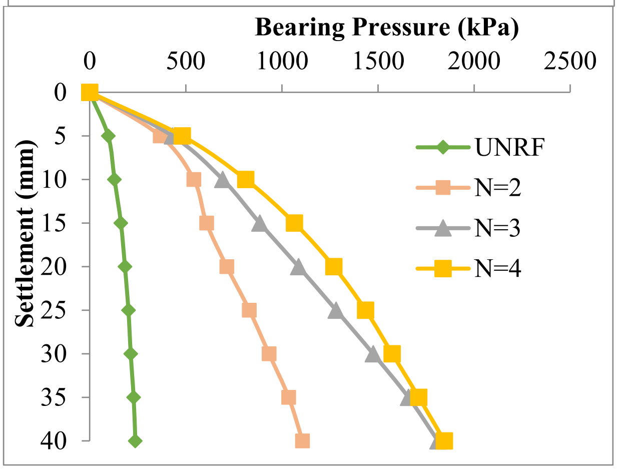

Fig.8 Pressure-settlement curves for square footing resting on geogrid reinforced M-Sand Bed with S=0.3B

Fig.9 Pressure-settlement curves for square footing resting on geogrid reinforced M-Sand Bed S=0.4

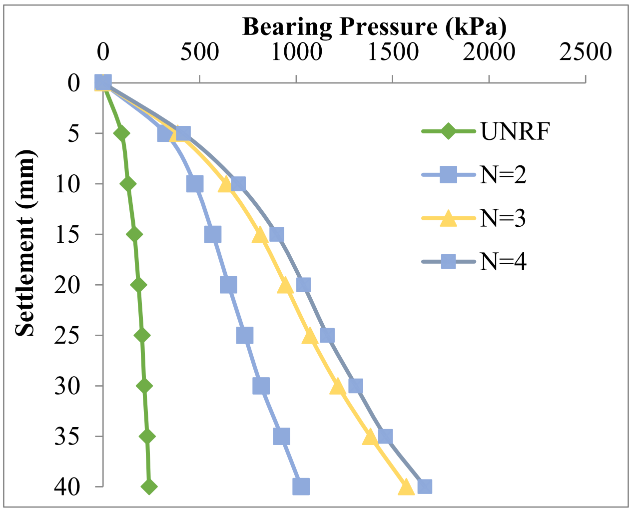

Fig.10 Pressure-settlement curves for square footing resting on geogrid reinforced M- Sand Bed S=0.5B

4.4 Finite Element modelling

Numerical simulations were performed using the ABAQUS 2023 to validate the experimental results. The software provides a range of material models, including linear elastic, elastoplastic, and viscoelastic formulations, enabling accurate representation of material behaviour. Within the finite element framework, stresses and strains are evaluated at nodal points, making appropriate element selection and mesh refinement essential for reliable results. ABAQUS is widely employed for solving both linear and nonlinear problems and supports implicit as well as explicit analysis procedures, making it suitable for geotechnical applications.

4.4a M-sand parameters

The elasto-plastic behaviour of manufactured sand was modelled using the Drucker–Prager constitutive framework. The required material parameters include Young's modulus (E), Poisson's ratio (μ), friction angle (ϕ), cohesion (c), dilatancy angle (ψ), and unit weight (γ). These parameters were determined from laboratory testing of M-sand samples. In particular, cohesion (c), friction angle (ϕ), and Young's modulus (E) were obtained from direct shear tests, while Poisson's ratio was assumed as 0.3 for all cases. The equivalent Drucker–Prager friction parameter (β) was derived from the Mohr–Coulomb friction angle (ϕ) using the relationship $\tan\beta = (3\sqrt{3}\tan\phi') / \sqrt{(9 + 12\tan^2\phi')}$, corresponding to plane strain conditions. The dilatancy angle (ψ) was estimated using the empirical expression $\psi = \phi - 30°$, as proposed by Bolton (1986). The full set of input parameters adopted for the numerical simulations is presented in Tables 3.

Table 3: M-sand Properties

Sl. No	Properties	Results
1.	Relative density (%)	35
2.	Density, γ (kN/m³)	17.40
3.	Friction angle, β (degree)	42.66
4.	Young's Modulus, E (MPa)	20.00
5.	Poisson's ratio, μ	0.30
6.	Dilation angle, Ψ (degree)	4
7.	Cohesion, d (kPa)	0

4.4b Reinforcement parameters

Biaxial Hexagonal geogrid is used as reinforcement material. The parametrs of Reinforcement material used for the numerical analysis are Density(γ), Young's Modulus(E) and Poisson's Ratio(μ). The properties of these parameters are listed in Table 4.

Table 4: Geogrid parameters

Sl. No	Properties	Results
1.	Density, γ (kN/m³)	14.00
2.	Young's Modulus, E (MPa)	1480
3.	Poisson's ratio, μ	0.30
4.	Tensile strength (kN/m)	7.74

This study integrates experimental investigation with numerical simulation to examine the performance of square footings resting on both unreinforced and geogrid-reinforced M-sand beds. The load–settlement responses obtained from Laboratory model tests served as a benchmark for validating the numerical model. A three-dimensional finite element model was developed using ABAQUS. To improve computational efficiency, only one-quarter of the experimental domain was simulated by applying symmetry conditions, Fig.13 shows the numerical model dimensions of radius of 250 mm and a height of 360 mm. The mechanical behaviour of M-sand was represented using the Drucker–Prager yield criterion, which is well suited for granular materials. The footing was modelled as a rigid square plate with a thickness of 10 mm.Fig.14 shows the numerical model of reinforced M-sand bed. The geogrid reinforcement was defined as an independent component and positioned within the soil domain according to the required configuration. The interaction between the reinforcement and the surrounding soil was simulated using the embedded region approach, where the geogrid elements were constrained to follow the deformation of the host soil medium.

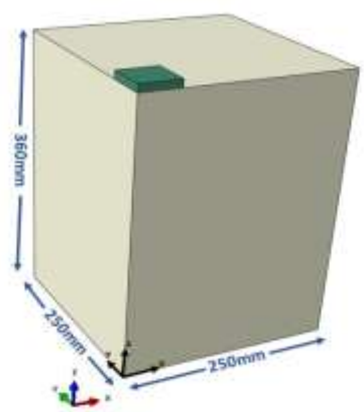

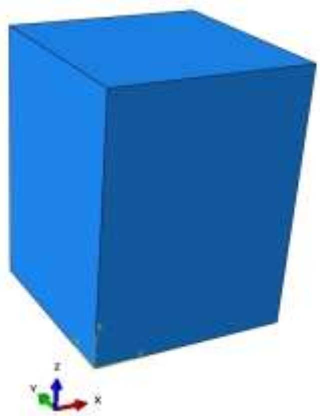
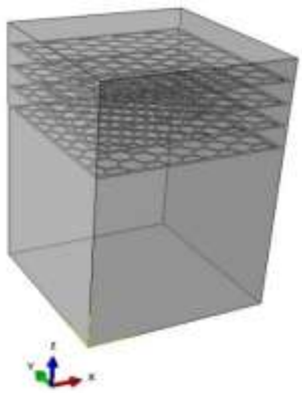

Fig.13 Numerical model dimension **Fig.14 Numerical model of reinforced M-sand bed (N=4)**

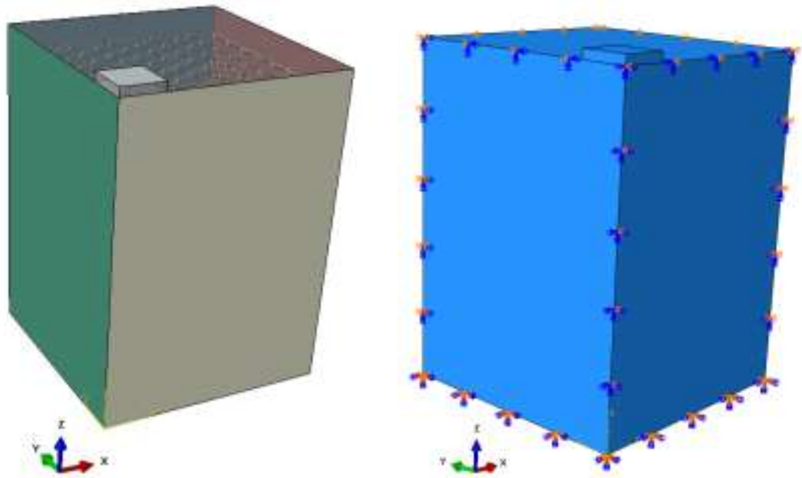

Fig. 15 Boundary conditions

4.4c Boundary conditions

A dynamic implicit analysis scheme was adopted under quasi-static loading conditions to simulate the response of the system. The load was applied incrementally to approximate static behaviour while ensuring numerical convergence and stability. The analysis was carried out in multiple stages, with each step representing a distinct phase of load application. Fig.15 Presents the adopted boundary conditions, which were defined to closely replicate realistic field constraints. The lateral boundaries were constrained against horizontal movement while allowing vertical displacement. Symmetry boundary conditions were applied along the designated planes to reduce computational effort, and the base of the model was fixed in all directions.

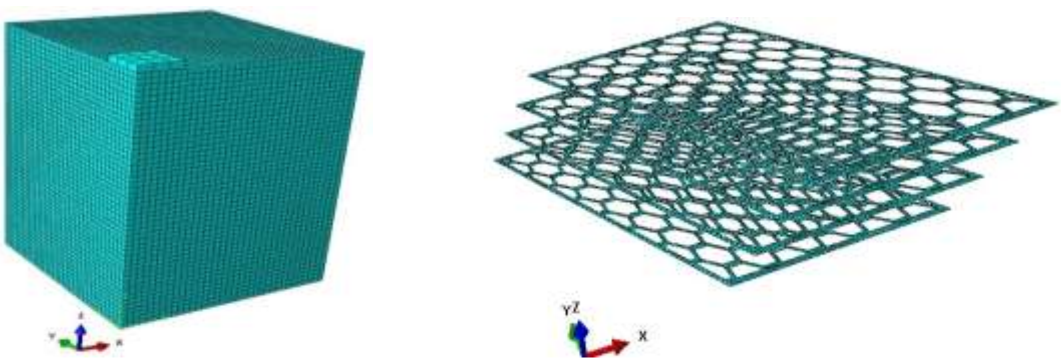

a) M-sand mesh using C3D8R elements **b) Geogrid mesh using S4R elements**

Fig. 16 Finite element mesh

4.4d Meshing

Fig.16 Presents the meshing strategy adopted for the numerical model. The soil domain was discretized using eight-node linear brick elements with reduced integration (C3D8R), which are well suited for simulating three-dimensional stress–strain behaviour. The geogrid reinforcement was modelled using four-node shell elements with reduced integration (S4R), providing an efficient representation of thin tensile inclusions within the soil mass.

4.5 Model Verification

To assess the accuracy of the developed numerical model, a three-dimensional finite element analysis was carried out using ABAQUS, and the results were validated against experimental observations for both unreinforced and geogrid-reinforced M-sand beds compacted at 35% relative density. Fig.17 and Fig.18

Presents the pressure–settlement behaviour of square footings resting on unreinforced and reinforced M-sand beds, respectively. A strong agreement between the numerical and experimental results is evident. For the unreinforced case (Fig. 17), the bearing pressure at a settlement of 40 mm was found to be 238 kPa experimentally and 225 kPa numerically, corresponding to a percentage deviation of approximately 5.46%. In the reinforced condition (Fig. 18), the experimental and numerical bearing pressures were 2223 kPa and 2251 kPa, respectively, yielding a deviation of about 1.26%. The relatively small differences between the results can be attributed to modelling simplifications, such as the assumption of homogeneous material properties and idealized boundary conditions. Nevertheless, the numerical model accurately captures the load–settlement response and overall behaviour of both reinforced and unreinforced systems. Based on the close correlation and low percentage error, the developed finite element model is considered reliable and was subsequently employed to perform a detailed parametric study. The analysis focused on evaluating the influence of reinforcement parameters, including the depth of the first reinforcement layer (U/B), spacing between reinforcement layers (S/B), and the number of reinforcement layers (N).

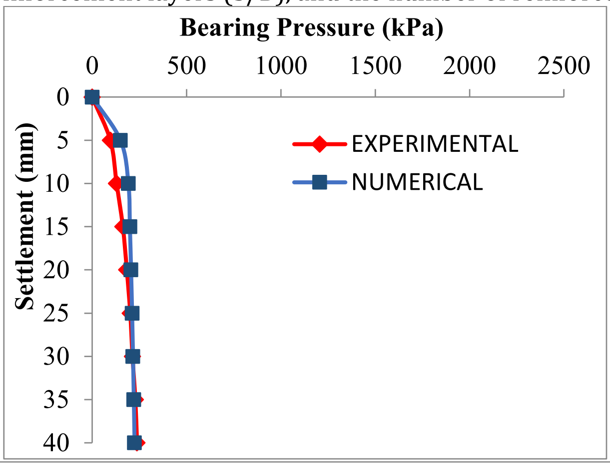

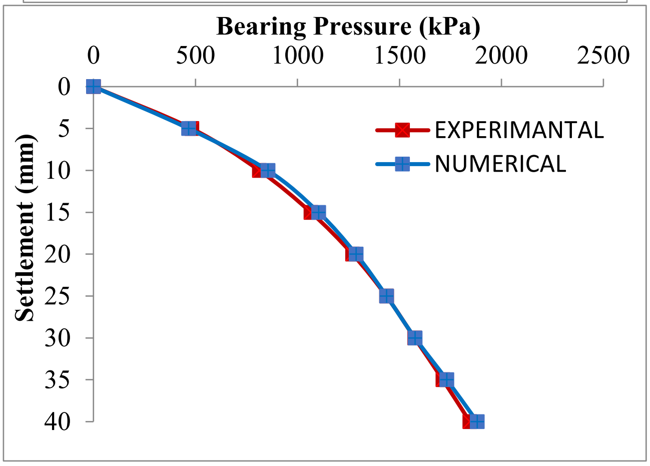

Fig.17 Pressure v/s Settlement curves for unreinforced
Fig.18 Pressure v/s Settlement curves for reinforced M-

4.6 Displacement contours of unreinforced and reinforced models

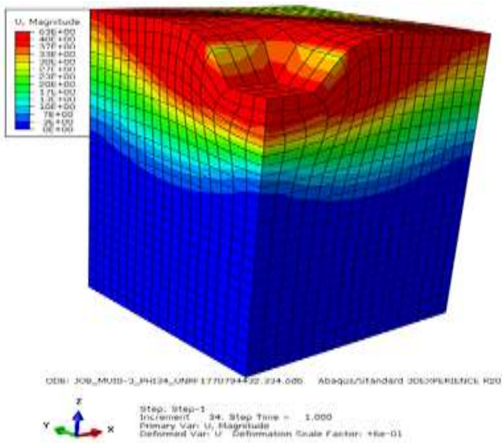

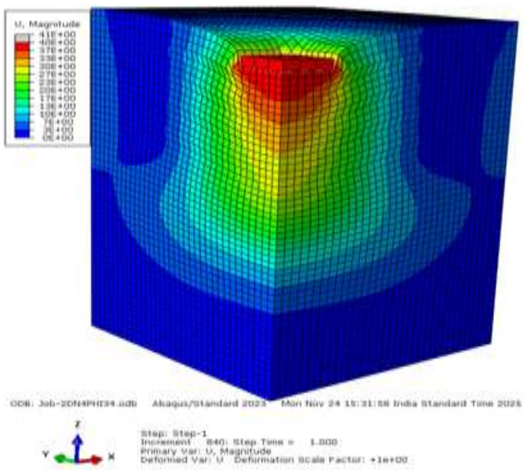

a. Unreinforced M-sand b.
Reinforced M-sand model with S/B=0.3

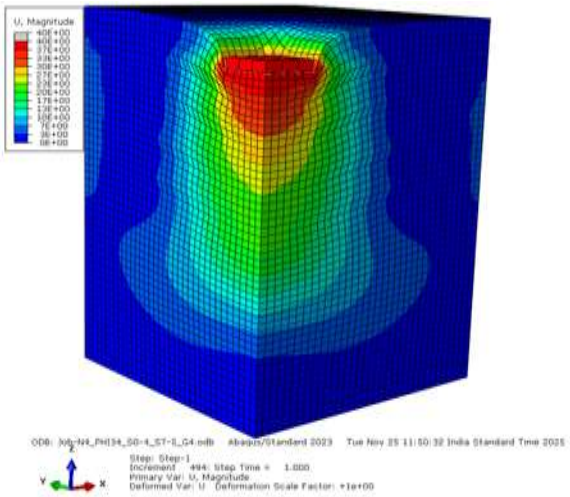

c. Reinforced M-sand model with S/B=0.4

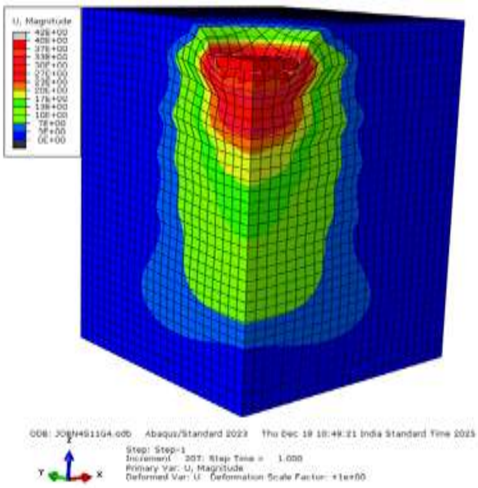

d. Reinforced M-sand model with S/B=0.5

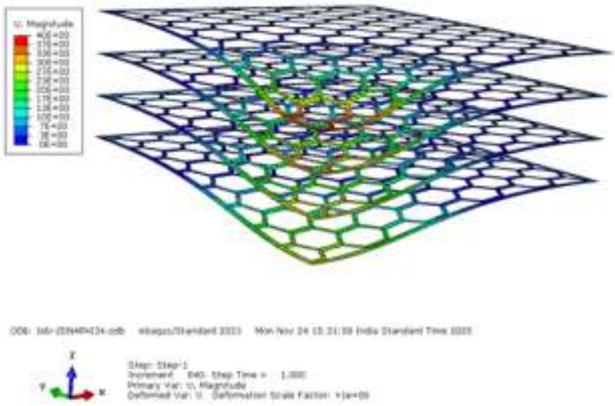

e. Deformation of geogrid

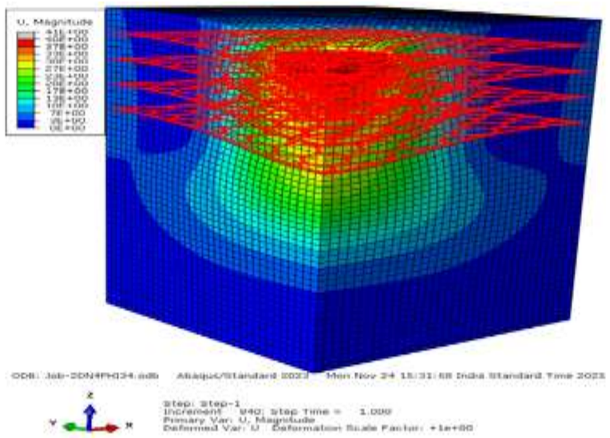

f. Deformation of geogrid reinforced M-sand

Fig.15(a-f) Displacement of footing resting on unreinforced and geogrid reinforced M-sand beds (U/B=0.3, S/B=0.3,0.4 and 0.5, N=4)

Fig. 15 (a)-(f) shows the displacement contours of unreinforced M-sand bed and reinforced M-sand bed with spacing of 0.3, 0.4 and 0.5 for N=4. It is observed that unreinforced M-sand bed shows larger deformation compared to reinforced M-sand beds. Reinforced M-sand bed with S/B=0.3 shows smaller deformation compared to S/B=0.4 and 0.5. The numerical results clearly demonstrate that the presence of geogrid layers alters the stress transfer mechanism by redistributing stresses laterally, resulting deeper pressure bulb compared to the unreinforced condition. It also observed that The contour plots represent the variation of displacement within the soil mass under applied loading, where red zones indicate maximum deformation and blue zones indicate minimal displacement.

In the case of the unreinforced M-sand bed, the displacement is highly concentrated directly beneath the footing. The deformation pattern shows a pronounced settlement zone extending vertically downward, forming a relatively narrow stress bulb. This indicates that the applied load is transferred primarily in the vertical direction, leading to higher localized settlement and reduced load distribution efficiency. With the inclusion of geogrid reinforcement layers, a significant modification in displacement behaviour is observed. The reinforced cases exhibit a wider and more distributed deformation pattern. The presence of geogrid layers restricts vertical deformation and promotes lateral spreading of stresses. As a result, the settlement beneath the footing is reduced, and the stress distribution becomes more uniform across a larger soil volume.

As the number of geogrid layers increases, the confinement effect within the M-sand improves further. The displacement contours become broader and less intense, indicating enhanced stiffness of the composite soil–geogrid system. The reinforcement layers act as tension-resisting elements, reducing the concentration of stresses and preventing excessive deformation. The image showing multiple geogrid layers separately highlights their deformation profile, demonstrating that the reinforcement layers undergo tensile strain and interact effectively with the surrounding soil. The embedded action between soil and geogrid ensures composite behaviour, which contributes to improved load-carrying capacity. In the final reinforced configuration, the deformation zone becomes wider and shallower compared to the unreinforced case. This clearly indicates that the geogrid reinforcement alters the load transfer mechanism, resulting in reduced settlement, improved stress distribution, and enhanced overall performance of the foundation system.

4.7 Comparison of numerical modelling results with experimental results

Table 3 and Fig.16 shows the comparison of experimental results and numerical results of load bearing pressure for footing on reinforced M-sand bed with depth of first layer of reinforcement U/B = 0.3, 0.4 and 0.5. The percentage of variation in experimental and numerical results are with in a deviation of ± 6%.

Table 4 and Fig.17 shows the comparison of experimental results and numerical results of load bearing pressure for reinforced M-sand bed with numbers of reinforcement layers N=2, 3 and 4 with a reinforcement spacing of 0.3B. The percentage of variation in experimental and numerical results is with less then ± 6%, Similarly, Table 5 and Fig.18 and Table 6 and Fig.19 shows the comparison of experimental results and numerical results of load bearing pressure of reinforced M-sand bed for numbers of reinforcement layers N=2, 3 and 4 with spacing between the reinforcement layers S/B = 0.4 and 0.5 respectively. The percentage of variation in experimental and numerical results is less than ± 6%, This validation conclude that both experimental results and numerical results are in close agreement.

Table 7 and Fig.20 shows the comparison of experimental results and numerical results of load bearing pressure for two layered reinforced M-sand bed with spacing between the reinforcement layers S/B= 0.3, 0.4 and 0.5. The percentage of variation in experimental and numerical results is less than ± 6%, Similarly, Tables 8 and 9, along with Fig. 21 and 22 shows the comparison of experimental results and numerical results of load bearing pressure for three and four layered reinforced M-sand beds with spacing between the reinforcement layers S/B = 0.3, 0.4 and 0.5. The percentage of variation in experimental and numerical results is ± 6%.

Table 3. Bearing pressure footing resting on unreinforced and geogrid reinforced M-sand beds with different U/B

Condition	Bearing Pressure		Percentage of Variation
	Computed value (kPa)	Experimental value(kPa)	
Unreinforced	225	238	-5.77
U/B=0.3	681	672	1.32
U/B=0.4	636	615	3.30
U/B=0.5	594	561	5.55

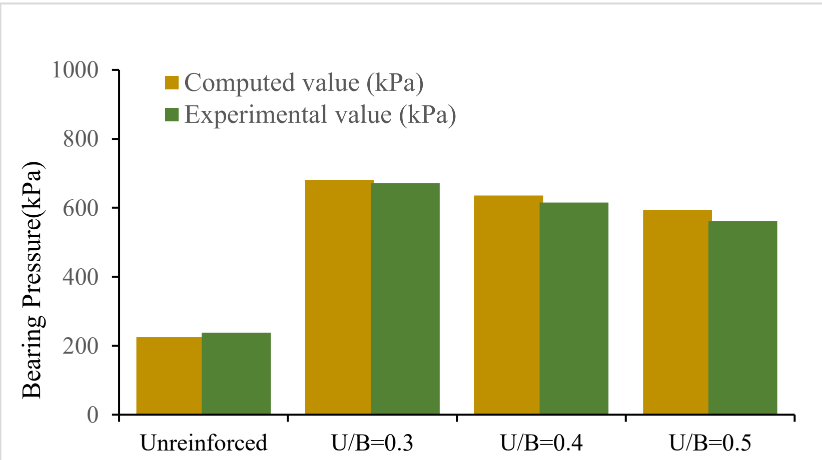

Fig. 16. Comparison of bearing pressure of footing resting on unreinforced and geogrid reinforced M-sand beds with different U/B

Table 4. Bearing pressure of footing for different number of layers of geogrid reinforcement (N) for S=0.3B

Number of geogrid reinforced layers (N)	Bearing Pressure		Percentage of Variation
	Computed value (kPa)	Experimental value (kPa)	
Unreinforced	225	238	-5.77
N=2	1431	1391	2.79
N=3	1869	1824	2.40
N=4	2223	2251	-1.25

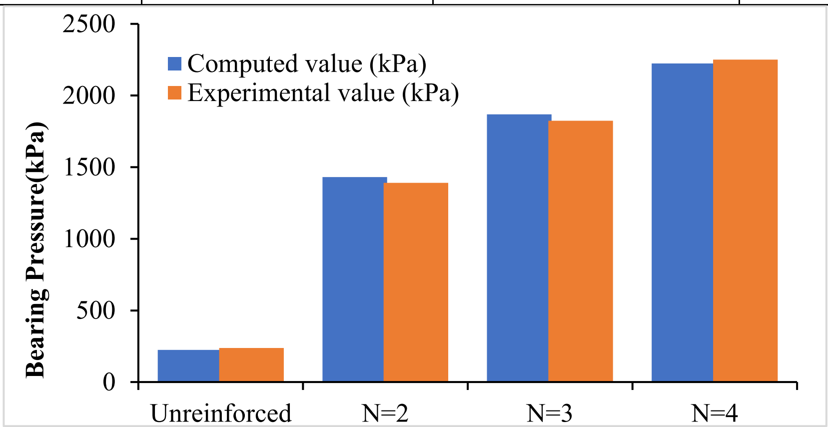

Fig. 17. Comparison of bearing pressure of footing resting on geogrid reinforced M-sand bed with different number of reinforcement layers at S=0.3B

Table 5. Bearing pressure of footing for the different number of layers of geogrid reinforcement (N) for S=0.4B

Number of geogrid reinforced layers (N)	Bearing Pressure		Percentage of Variation
	Computed value (kPa)	Experimental value (kPa)	
Unreinforced	225	238	-5.77
N=2	1131	1108	2.03
N=3	1794	1812	-1.00
N=4	1881	1845	1.91

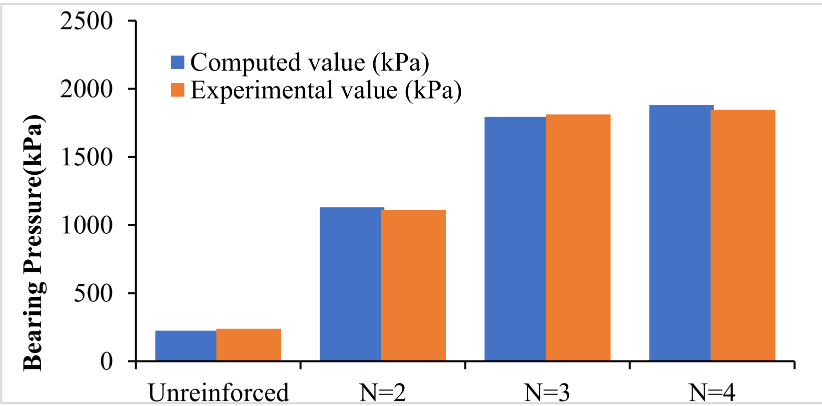

Fig. 18. Comparison of bearing pressure of footing resting on geogrid reinforced M-sand bed with different number of reinforcement layers at S=0.4B

Table 6. Bearing pressure of footing for the different number of layers of geogrid reinforcement (N) for S=0.5B

Number of geogrid reinforced layers (N)	Bearing Pressure		Percentage of Variation
	Computed value (kPa)	Experimental value(kPa)	

Unreinforced	225	238	-5.77
N=2	1117	1026	8.14
N=3	1660	1571	5.36
N=4	1758	1668	5.11

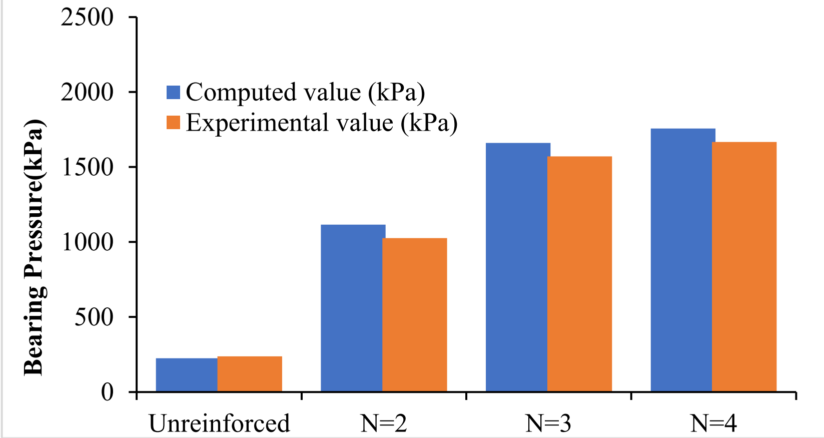

Fig. 19. Comparison of bearing pressure of footing for the different number of layers of geogrid reinforcement (N) for S/B=0.

Table 7. Bearing pressure of footing for the spacing between the geogrid reinforcement layers for N=2 layers

Spacing between the reinforced layers	**Bearing Pressure**		**Percentage of Variation**
	Computed value (kPa)	**Experimental value (kPa)**	
Unreinforced	225	238	-5.77
S/B=0.3	1431	1391	2.79
S/B=0.4	1131	1108	2.03
S/B=0.5	1117	1026	8.14

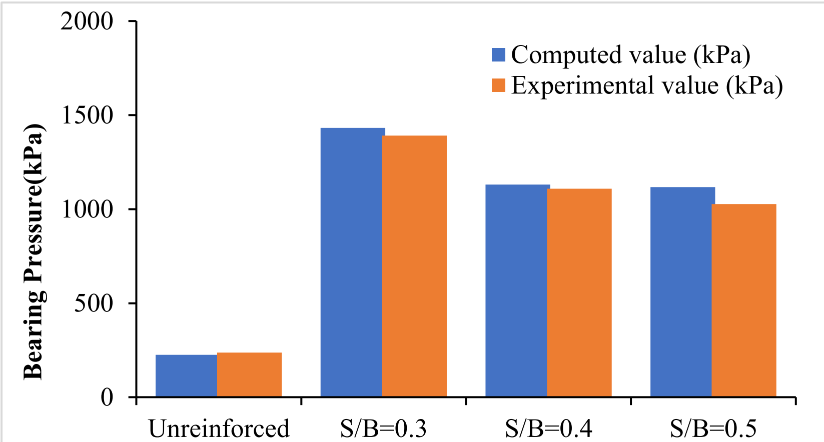

Fig. 20. Comparison of bearing pressure resting on geogrid reinforced M-sand bed with different reinforcement spacing (N=2)

Table 8. Bearing pressure of footing for the spacing between the geogrid reinforcement layers for N=3 layers

Spacing between the reinforced layers	**Bearing Pressure**		**Percentage of Variation**
	Computed value (kPa)	**Experimental value (kPa)**	
Unreinforced	225	238	-5.77
S/B=0.3	1869	1824	2.40
S/B=0.4	1794	1812	-1.00
S/B=0.5	1660	1571	5.36

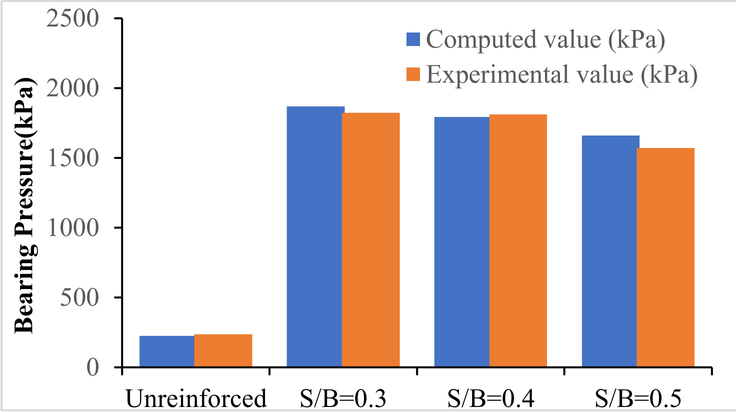

Fig. 21. Comparison of bearing pressure resting on geogrid reinforced M-sand bed with different reinforcement spacing (N=3)

Table 9. Bearing pressure of footing for the spacing between the geogrid reinforcement layers for N=4 layers

Spacing between the reinforced layers	Bearing Pressure		Percentage of Variation
	Computed value (kPa)	Experimental value (kPa)	
Unreinforced	225	238	-5.77
S/B=0.3	2223	2251	-1.25
S/B=0.4	1881	1845	1.91
S/B=0.5	1758	1668	5.11

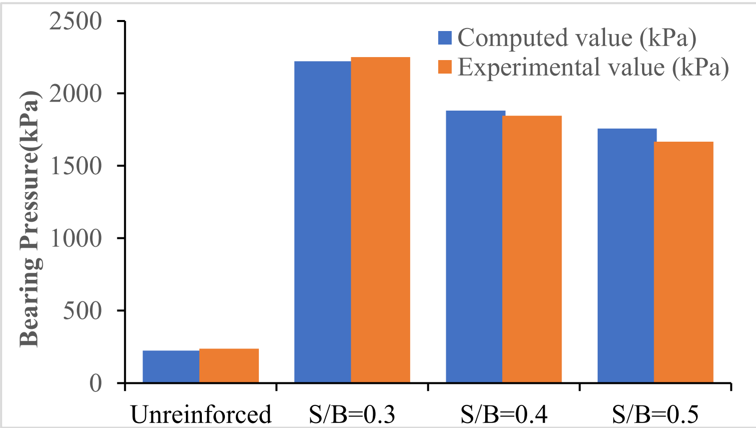

Fig. 22. Comparison of bearing pressure resting on geogrid reinforced M-sand bed with different reinforcement spacing (N=4)

5. Conclusion

Based on the results of experiments conducted and the results of numerical analysis the following conclusions are drawn:

- Square footing resting on reinforced M-sand beds exhibited improved performance compared to those on unreinforced sand beds, irrespective of the number of reinforcement layers and the spacing between them under static loading conditions.
- The depth of first layer of reinforcement from the footing level is found to be effective at 0.3 times the width of the footing (i.e., U=0.3B) for geogrid reinforced condition.
- A reinforcement spacing of S=0.3B shows the maximum bearing capacity ratio along with minimum settlement ratio hence it is concluded that the optimum spacing of reinforcement layers is 0.3B.
- An increase in the number of reinforcement layers (N) in the M-sand bed leads to increase in the bearing pressure of the footing. Based on the present test results, the provision of four geogrid layers was found to yield the optimum performance.
- The numerical study confirms that ABAQUS is a suitable and an efficient tool for analyzing the behavior of geogrid-reinforced sand beds and can be reliably used for parametric studies

6. References

1. Avinash Bhardwaj, Ravi Kumar Sharma (2023).: "Bearing Capacity Evaluation of Shallow Foundations on Stabilized Layered Soil using ABAQUS" Studia Geotechnica et Mechanica, 2023; 45(1): 55–71 (2023)
2. Adel Belal ,Nabil Nagy, Ahmed Elshesheny (2015) "Numerical Evaluation of Bearing Capacity of Square Footing on Geosynthetic Reinforced Sand"Proceedings of the International Conference on Civil, Structural and Transportation Engineering Ottawa, Ontario, Canada, May 4 – 5, 2015.
3. Ahmed M. Gamal, Adel M. Belal, S. A. Elsoud, (2016) " Numerical Modeling of Geogrid Reinforced Soil Bed under Strip Footings using Finite Element Analysis" World Academy of Science, Engineering and Technology,International Journal of Civil and Environmental Engineering Vol:10, No:1, 2016
4. Ahmed Elshesheny, Ahmed Badawy, Nabil Nagy (2014).: "Finite Element Analysis of Square Footing Resting on Geosynthetic Reinforced Soil" https://www.researchgate.net/publication/308971765 (2014)
5. Aminaton Marto, Mohsen Oghabi And Nor Zurairahetty Mohd Yunus (2015).: "Bearing capacity of Circular footing on Sand Deposit" © 2015 The Author(s). Published by Trans Tech Publications Ltd, Switzerland (2015).
6. Anand Shrigondekar and Prabhuling Ullagaddi (2020).: "Bearing Capacity Analysis of a Square Footing Supported on Geogrid Reinforced Sand" International Journal on Emerging Technologies
7. Binquet, J and Lee, K.L. (1975) "Bearing capacity analysis of reinforced earth mass" Journal of Geotechnical Engineering, Div, ASCE, 101(12), 1241-55.
8. Computedy M. Makkar, Sreya M.V. (2022).: "Numerical Modelling of the Behaviour of 3D Geogrid Reinforced Soil Foundation" www.jetir.org (ISSN-2349-5162) (2022)
9. Gaurav Juneja, Ravi Kumar Sharma (2022).: "Numerical Investigation Of Square Footing Positioned On Geocell Reinforced Sand By Using Abaqus Software" Civil Engineering Department, NIT Hamirpur (HP), India, e-mail: juneja.gaurav@nith.ac.in
10. Mabrouk Touahmia, Ahmed Rouili, Mustapha Boukendakdji, Belkacem Achour (2018).: "Experimental and Numerical Analysis of Geogrid-Reinforced Soil Systems" Arabian Journal for Science and Engineering https://doi.org/10.1007/s13369-018-3158-6 (2018)
11. Rojimol J, and Umashankar B (2022).: "Three-Dimensional Analysis Of Geogrid Reinforced Flexible Pavement Using Finite Difference Program Flac3d" International Journal of GEOMATE, April, 2022, Vol.22, Issue 92, pp.41-47 (2022)
12. Roma Sahu, C. R. Patra, Nagaratnam Sivakugan (2015).: "Ultimate bearing capacity of rectangular foundation on geogrid-reinforced sand under eccentric load" International Journal of Geotechnical Engineering · May 2015.
13. Sagar Chhetri and Plaban Deb (2024).: "Finite Element Analysis of Geogrid-Incorporated Flexible Pavement with Soft Subgrade" https://www.mdpi.com/journal/applsci (2024)
14. Shaziya Banu, Mousa Attom, Farid Abed, Ramesh Vandanapu, Philip Virgil Astillo, Naser Al-Lozi and Ahmed Khalil (2024).: "Numerical Analysis of the Ultimate Bearing Capacity of Strip Footing Constructed on Sand-over-Clay Sediment" https://www.mdpi.com/journal/buildings (2024).
15. Salahudeen, A. B. and Sadeeq, J. A (2016).: "Numerical Modelling Of Soil Reinforcement Using Geogrids" Proceedings of the Fourth International Conference on Engineering and Technology Research February 23 - 25, 2016 ISBN: 978-2902-58-6 Volume 4 (2016)
16. SIMULIA (2023) ABAQUS analysis user's manual.